AIMS Materials Science, 9(2): 297–310.
DOI: 10.3934/matersci.2022018
Received: 20 December 2021
Revised: 02 March 2022
Accepted: 03 March 2022
Published: 17 March 2022

http://www.aimspress.com/journal/Materials

Research article

Tuning the giant Magnetocaloric Effect and refrigerant capacity in $Gd_{1-x}Y_xCrO_3$ ($0.0 \leq x \leq 0.9$) perovskites nanoparticles

Imaddin A. Al-Omari[1,*], Muna D. Al-Mamari[1] and D.J. Sellmyer[2]

[1] Department of Physics, PO Box 36, Sultan Qaboos University, PC 123 Muscat, Oman
[2] Nebraska Center for Materials and Nanoscience and Department of Physics and Astronomy, University of Nebraska, Lincoln, Nebraska 68588, USA

* **Corresponding author**: Email: ialomari@squ.edu.om.

Abstract: Different compounds of rare-earth orthochromites $Gd_{1-x}Y_xCrO_3$ (where x is 0.0–0.9) powder nanoparticles, were synthesized by the auto-combustion method followed by annealing at 700 ℃. All the compounds showed single-phase and crystallized into a distorted orthorhombic structure with the space group (Pbnm). The average particle size for all the samples were in the range 53–110 nm. The detailed and systematic magnetic measurements and analysis showed that all the samples up to x = 0.9 have large magnetization and large values of the change in the magnetic entropy. The magnitude of the change in the magnetic entropy (at 4.5 K and for all the values of the change in the applied magnetic field between 1 and 9 T) is found to increase with increasing x reaching a maximum value at x = 0.3 then it decreases as we increase the yttrium concentration. The nanoparticle compounds with low yttrium concentrations showed a giant change in the magnetic entropy and a giant relative cooling power. Based on the slopes of Arrott plots curves the order parameter of the magnetic transition has been estimated and found to be second order. The giant change in the magnetic entropy and the relative cooling power were tuned in the rages (−45.6 to −8.7 J/kg·K at a change in the applied magnetic field of 9 T; and 136–746 J/kg), around the helium liquefaction temperature. The magnitude of the change in the magnetic entropy is significantly larger for large range of temperatures, up to the nitrogen liquefaction temperature. The giant change in the magnetic entropy and the giant relative cooling power at low temperatures (in the range about 4 to 20 K.) make

these samples candidate materials for the low temperature magnetic refrigerant applications, based on the magnetocaloric effect.

Keywords: giant magnetocaloric effect; magnetic entropy; relative cooling power; refrigerant capacity; gadolinium-yttrium chromites; Arrott plots

1. Introduction

Magnetic refrigeration based on the magnetocaloric effect (MCE) has attracted increasing interest in recent years due to the clean energy feature and it can be an alternative to conventional vapor compression refrigeration [1]. "The MCE, which is an intrinsic property of magnetic materials, is defined as the thermal response (heating or cooling) of magnetic solids during the application or removal of an external magnetic field" [2]. For temperatures below the critical temperature of the magnetic phase transition, the magnetic moments can be aligned by applying external magnetic field on the material. During this process the magnetic entropy (S_M) of the material (under the adiabatic conditions) decreases because of the moments ordering and to compensate for the decrease in the magnetic entropy the lattice entropy (under the adiabatic conditions) increases, which causes an increase in the temperature [3].

Rare-earth orthochromites $RCrO_3$ (where R = Y or trivalent rare-earth ion) are a class of interesting materials which showed various magnetic properties for example magnetization Reversal (MR), spin reorientation (SR), change in the magnetic entropy (ΔS_M), and exchange bias (EB) [4–9]. These different magnetic properties are temperature and magnetic-field-controlled which makes them potential materials for many applications such as spintronics, magnetic switches, thermally assisted random access memory devices, magnetic refrigeration based on the magnetocaloric effect [10–13].

In the recent years, many researchers focused on the search for magnetic materials with large change in the magnetic entropy (ΔS_M) and large values of the relative cooling power (RCP). The $RCrO_3$ perovskite compounds have canted antiferromagnetic structure where Cr^{3+} ions occupy the octahedral sites and they are coupled antiparallel with slight canting of Cr^{3+} ions, resulting in week ferromagnetic below the critical Néel temperature. The interaction between the internal magnetic field produced by Cr^{3+} ions and the magnetic moments of the trivalent rare-earth ions can be weak or strong depending on the trivalent rare-earth ion and the temperature, and at certain range of temperatures spin reorientation occurs. Mahana et al. [14] studied the magnetic properties of polycrystalline $GdCrO_3$ prepared by solid-state technique, followed by annealing at 1400 °C. They found that this compound "exhibits a giant magnetocaloric effect (MCE) with a maximum entropy change of 36.97 J/kg·K, a diabatic temperature change of 19.12 K and a refrigeration capacity of 542 J/kg for a field change of 7 T at low temperatures". The $GdCrO_3$ single crystal was grown with the laser-diode-heated floating-zone technique have been studied by Zhu et al. [15] and they found that ($-\Delta S_M$) is about 57.5 J/kg·K at 6 K and at a change in the applied magnetic field of 14 T. Oliveira et al. [16,17] studied the "effect of chemical pressure on the magnetocaloric effect of perovskite-like, $RCrO_3$ (R-Yb, Er, Sm and Y)" and the MCE in $YCrO_3$. They found that for $YCrO_3$ the magnitude of the change in

the magnetic entropy is equal to 3.5 at a temperature about 141 K and a change in the external magnetic field of 5 T.

In most of the published work, the researchers use solid-state reaction techniques, hydrothermal, or ball-milling to prepare their $RCrO_3$ samples. These methods usually take long time for the preparation and it needs high temperatures (≈1400 ℃) and long times (≈24–48 h) for sintering, which results in polycrystalline samples with particle sizes in the micrometer range. Although the findings of our recent research have not yet been formally published, the results are encouraging. Where we recently succeeded in preparing $Gd_{1-x}Y_xCrO_3$ nanoparticles using the very simple auto-combustion method followed by annealing at lower temperatures and shorter times (700 ℃ and for 4 h). First, we have in detail structural, magnetic, and morphological measurements, analysis and discussion about the effects of Y substitution for Gd on the magnetic and structural properties of $Gd_{1-x}Y_xCrO_3$ nanoparticles. And all the samples are canted antiferromagnetic (below the Néel transition temperature, T_N), and exhibit large exchange bias, and negative magnetization at low temperatures (≈110–10 K), which is responsible about the magnetic switching behavior in that temperature range. Changes in some of the magnetic properties is found due to the Y substitution for Gd, where the coercive field increases as we increased x reaching the maximum value (of 4.8 kOe) for the compound with x = 1.0 at a temperature of 125 K. For low temperatures (2–10 K) the coercive field is small (0.3 kOe, for x = 0) and it increases linearly by a small amount reaching 1.5 kOe for x = 0.9. In addition to that the magnitude of the exchange bias field increases as we increased the yttrium concentration, x, reaching a maximum at x = 0.7 then decreases. The increase in the magnitude of the exchange bias field was found to depend on the temperature for each compound. And we found that T_N = 171 ±2 K for x = 0 which is close to T_N = 171–177 K for polycrystalline $GdCrO_3$ compound [18–21], we also found that T_N decreases linearly with increasing the yttrium concentration reaching 146 ±2 K for x = 0.9. In addition, we found that T_{SF} = 14 ±2 K for x = 0 which is close to T_{SF} = 12 ±2 for polycrystalline compound [22–25], we also found that T_{SF} decreases linearly (by small amount) with increasing the yttrium concentration reaching 5 ±2 K for x = 0.9, indicating that the magnetocaloric effect in $GdCrO_3$ can be manipulated via Y-substitution.

In this paper, we present the results of a detailed temperature and field dependent magnetization and systematic study of the effect of yttrium substitution in $Gd_{1-x}Y_xCrO_3$ on the magnetic and magnetocaloric properties of the prepared nanoparticle compounds.

2. Materials and methods

Different nanoparticle powder samples of $Gd_{1-x}Y_xCrO_3$ (where x = 0.0, 0.3, 0.5, 0.7, and 0.9) were synthesized by the auto-combustion method, using glycine as fuel and nitrates as oxidants, followed by annealing at 700 ℃. X-ray diffraction measurements (XRD) were performed by using (PANalytical X' Pert, UK). The average particle size was determined from the images of the high-resolution transmission electron microscope. The magnetic measurements were done using a vibrating sample magnetometer (VSM), attached to a Dynacool Physical Property Measuring System (PPMS, Quantum Design, USA) in magnetic fields up to 9 T and in the temperature range of (2–300) K.

3. Results and discussion

Figure 1 shows the x-ray diffraction pattern with the Rietveld-fitting for $Gd_{0.5}Y_{0.5}CrO_3$. As we see from the figure that the sample has a single-phase and crystallized into a distorted orthorhombic structure and all the peaks in the diffraction pattern are indexed based on the space group (Pbnm). The crystallite size was calculated from the width of the different peaks and the average value is found to be (54 ±5) nm. All the other samples in this study showed similar diffraction patterns with very small shifts in the peak's positions due to the very small change in the unit cell volume, and different values of the average crystallite sizes.

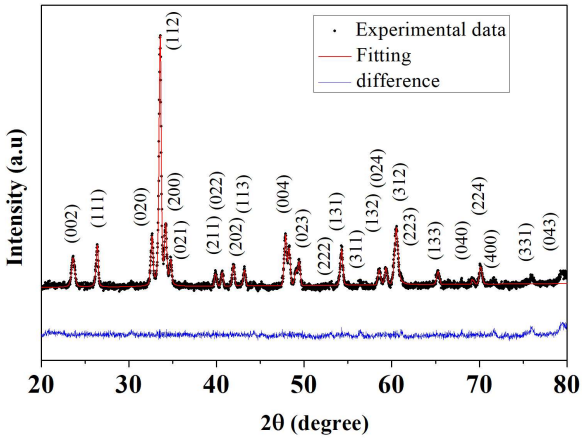

Figure 1. X-ray diffraction pattern for $Gd_{0.5}Y_{0.5}CrO_3$. The solid red line represents the Rietveld-fitting and the solid blue line represent the difference between the fitting and the experimental data.

The morphology and the microstructure of the samples were investigated from the micrographs of the TEM images. Figure 2 shows the image for a representative sample, $Gd_{0.5}Y_{0.5}CrO_3$. The image shows that most the nanoparticles have spherical shape with an average diameter of about (55 ±6) nm. The other samples under investigation showed similar images with an average diameter between 53 and 110 nm.

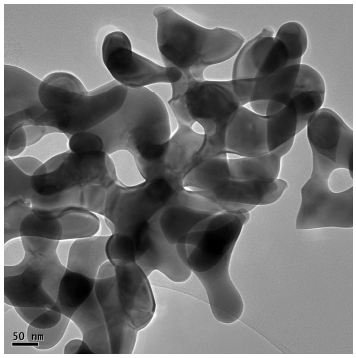

Figure 2. High-resolution TEM image for $Gd_{0.5}Y_{0.5}CrO_3$.

Figure 3 shows the isofield magnetization versus temperature curves during the zero field cooled (ZFC) and the field cooled (FC) modes at an applied magnetic field of 200 Oe for a representative sample with x = 0.5. It is clear from Figure 3 that the sample is paramagnetic above the Néel transition temperature, T_N, and it is canted antiferromagnetic (or weak ferromagnetic) below T_N with different magnetic features. Between the two compensation temperatures (T_{comp}-1 and T_{comp}-2) the sample undergo a magnetization reversal, where the magnetization changes from positive to negative. Another interesting feature is observed at a temperature called "spin reorientation or flipping temperature (T_{SF})", where the Gd^{3+}–Cr^{3+} coupling is rotated to align the Gd^{3+} moments parallel to the applied magnetic field.

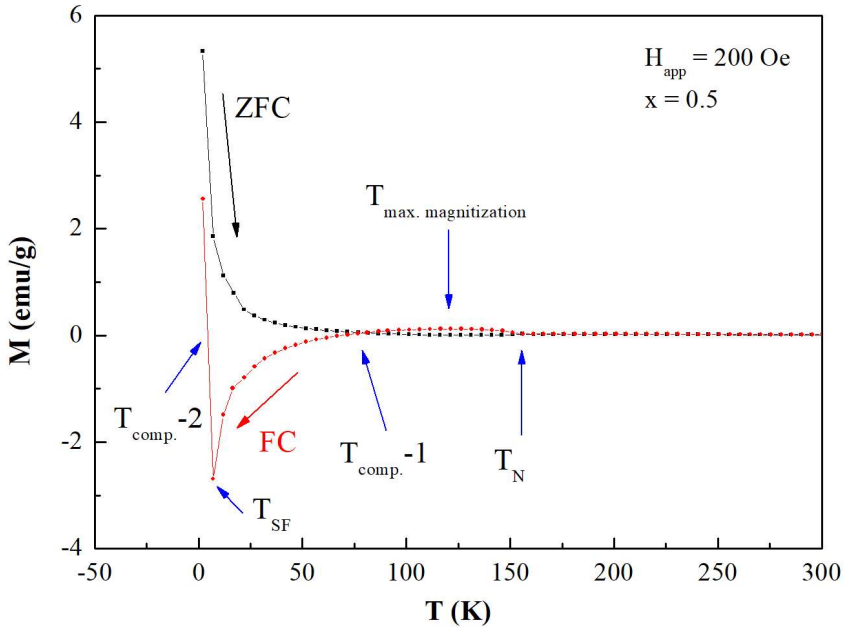

Figure 3. Isofield magnetization versus temperature curves during the zero field cooled (ZFC) and the field cooled (FC) modes at an applied magnetic field of 200 Oe for $Gd_{0.5}Y_{0.5}CrO_3$.

In order to investigate the magnetocaloric effect (MCE) and the relative cooling power, or refrigerant capacity, in $Gd_{1-x}Y_xCrO_3$ compounds we measured the dependence of the isothermal magnetization (M) on the applied magnetic field (μ_oH) at different temperatures. The applied magnetic field was increased in an isothermal manner from 0 to 90000 Oe in steps of 200 Oe. As we can see from Figure 4, at low temperature there is a visible curvature close to saturation (at the lowest temperatures) and as we increase the temperature the curvature decreases and also the magnetization decreases. In this study, the measured samples have a thin cylindrical shape and the applied magnetic field was along the length of the cylinder. We assumed that the internal magnetic field (H_{int}) is equal to the applied magnetic field (H_{app} or simply H) because the contribution to the internal field from the demagnetizing field (D) is negligible ($H_{int} = H_{app} - D \approx H_{app}$, where the maximum order of D is ≈ 60 Oe compared with 90000 Oe for the maximum H_{app}).

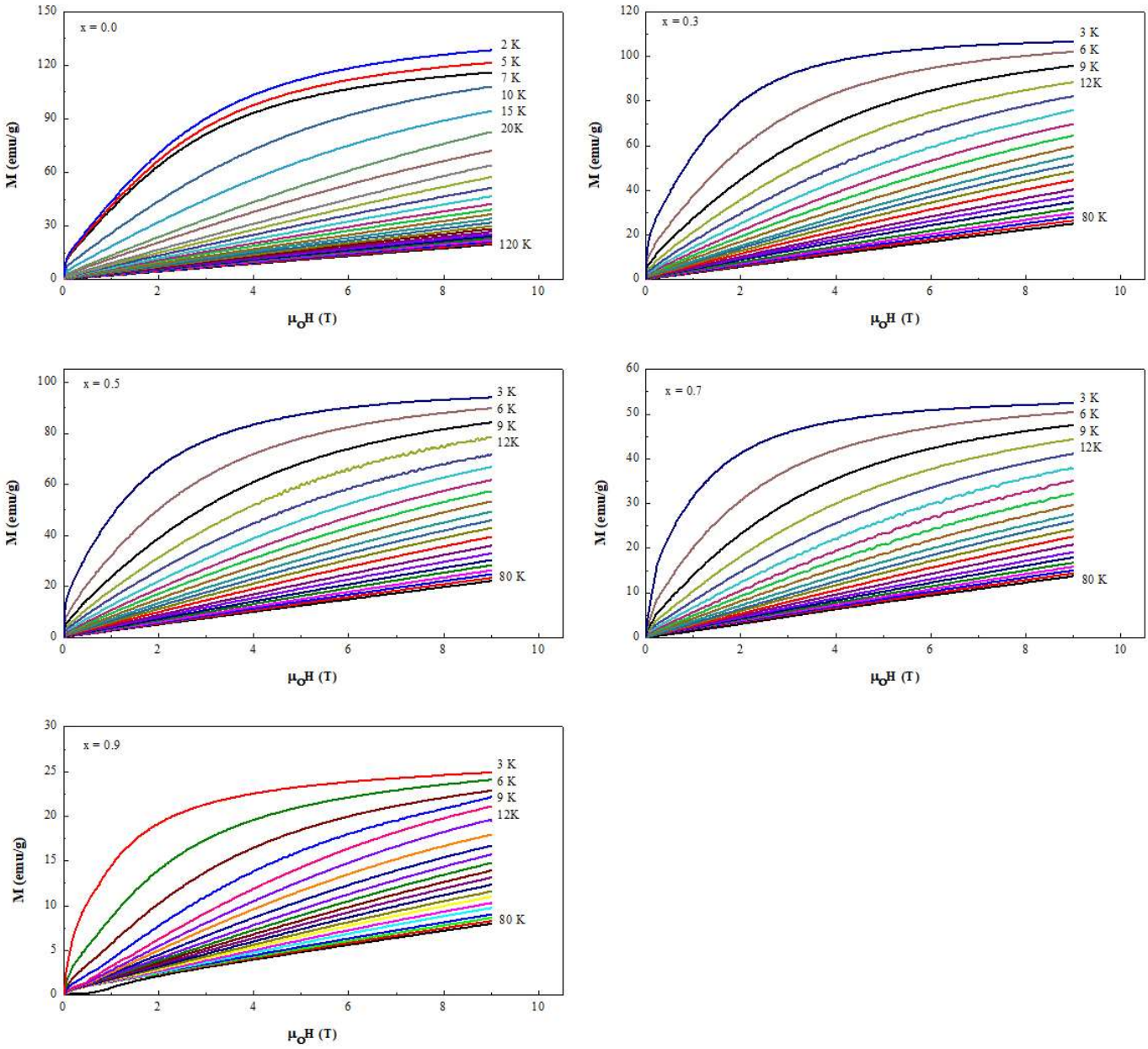

Figure 4. Dependence of the isothermal magnetization on the applied magnetic field at different temperatures for the different $Gd_{1-x}Y_xCrO_3$ ($0.0 \leq x \leq 0.9$) nanoparticle compounds.

The change in the magnetic entropy at a certain temperature and for a change in the applied magnetic field between 0 and H is found using Maxwell relation giving by Eq 1 [26,27]. ΔS_M were found at different temperatures between 4.5 and 77.5 K, and at different values of the change in the applied magnetic field between 1 and 9 T.

$$\Delta S_M(T, H) = \int_0^H \left(\frac{\partial M(T, H)}{\partial T}\right)_H .dH \quad (1)$$

Figure 5 shows the magnitude of the change in the magnetic entropy as a function of temperature and for different values of the change in the magnetic field (1 T ≤ $\Delta\mu_oH$ ≤ 9 T). The magnitudes of ΔS_M for all the samples above 50 K are relatively small and they are not shown in the figures, to make the figures clear for the readers. It is clear from the figure that for the compound with x = 0 the magnitude of the change in the magnetic entropy has a maximum at 8.5 K, while the other samples did not show any maximum in the temperature range from 4.5 to 77.5 K.

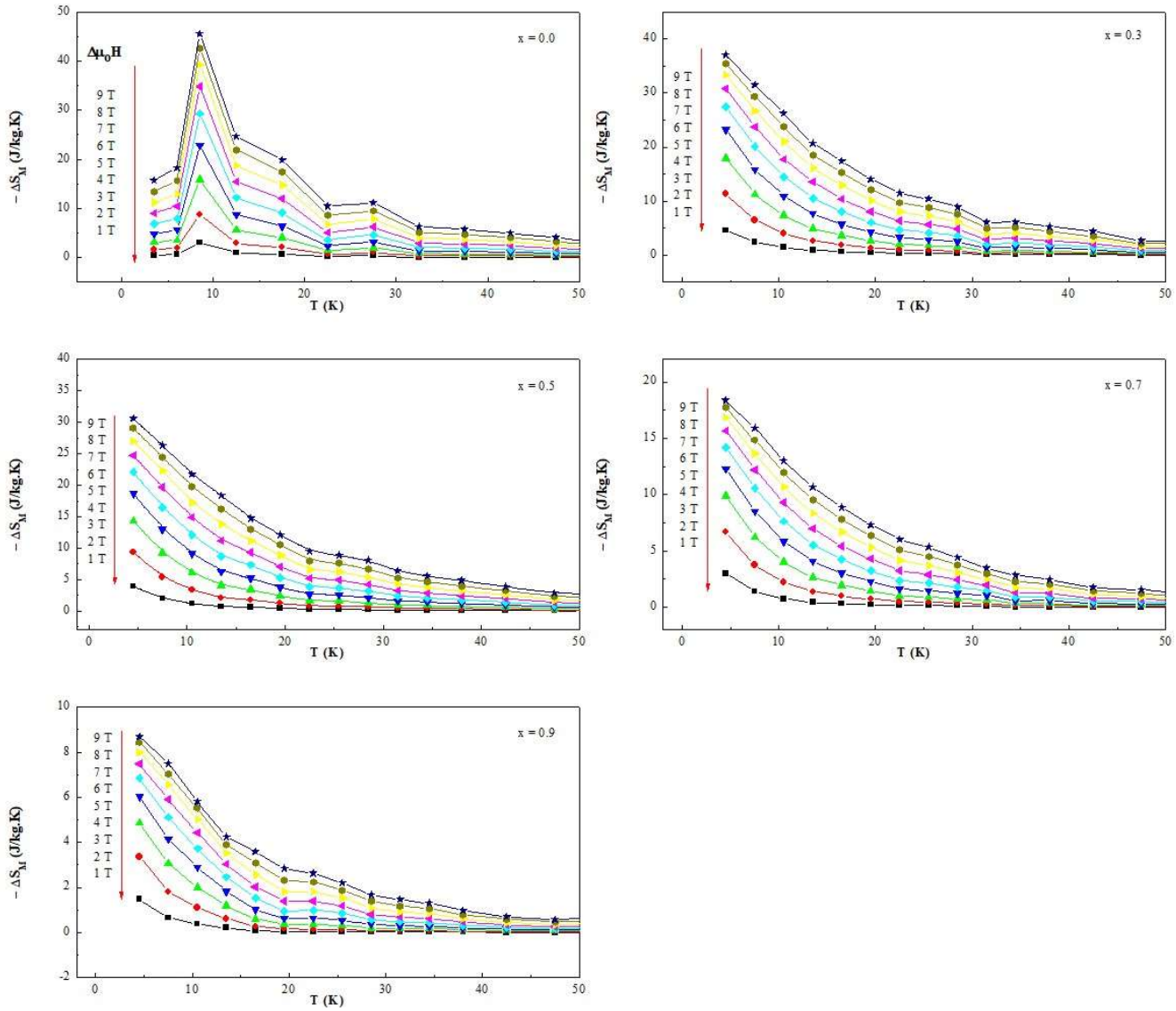

Figure 5. Dependence of negative the change in magnetic entropy on the temperature at different values of the change in the applied magnetic field for the different $Gd_{1-x}Y_xCrO_3$ ($0.0 \le x \le 0.9$) nanoparticles.

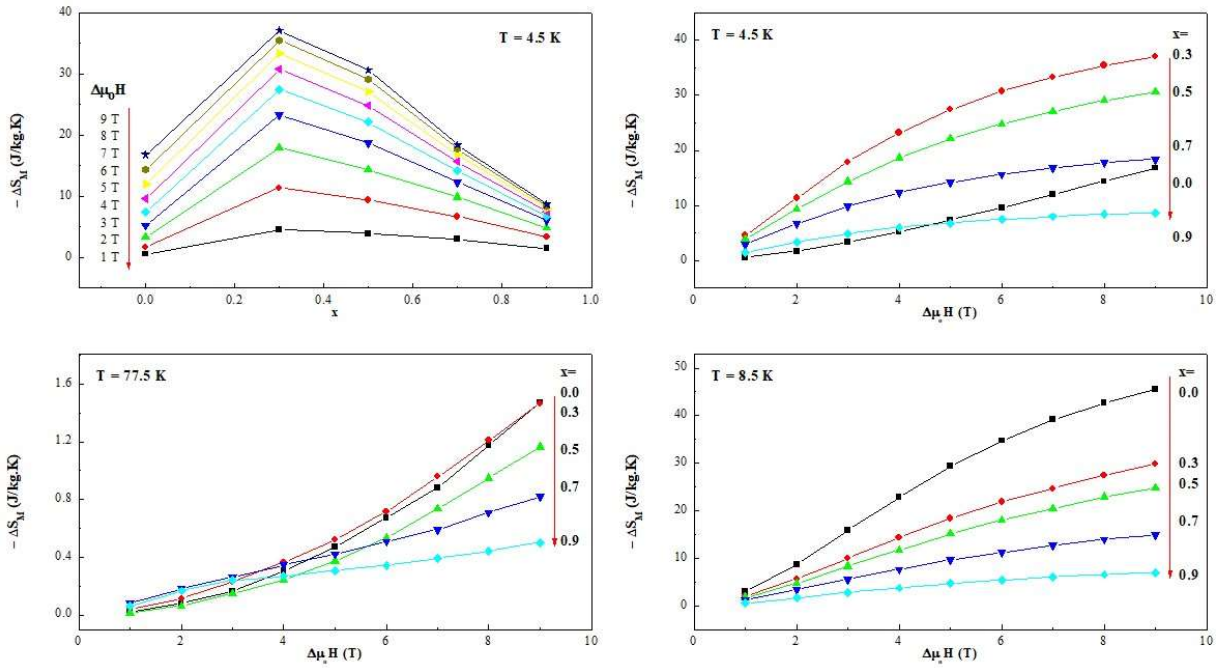

Figure 6. Dependence of negative the change in magnetic entropy on the Y composition (x) and on the different values of the change in the applied magnetic field ($\Delta\mu_oH$), at different temperatures T = 4.5, 8.5, and 77.5 K, for the different $Gd_{1-x}Y_xCrO_3$ ($0.0 \leq x \leq 0.9$) nanoparticles.

The dependence of negative the change in magnetic entropy ($-\Delta S_M$) on the yttrium composition (x) and on the different values of the change in the applied magnetic field ($\Delta\mu_oH$ = 1 to 9 T), at different temperatures T = 4.5, 8.5, and 77.5 K, for the different $Gd_{1-x}Y_xCrO_3$ ($0.0 \leq x \leq 0.9$) nanoparticles is illustrated in Figure 6. It is clearly seen from this figure that as we increase the change in the applied field the magnitude of the change in magnetic entropy increases. At T = 4.5 K, negative the change in magnetic entropy is found to increase with increasing the yttrium concentration in the compound reaching a maximum at x = 0.3 then decreases as we reduce the composition. The magnitude of ΔS_M showed the maximum value of 45.6 J/kg·K for x= 0.0 and μ_oH = 9 T at 8.5 K, which is the highest value for all the compounds under investigation. The wide temperature range of the magnitude of ΔS_M from 3.5 to 77.5 K, as shown in Figures 4 and 5, indicates an advantageous feature in the MCE field due to the nano-structuring of Gd-Y based oxide materials. This range in the temperature covers the cryogenic range from helium-liquefaction to nitrogen-liquefaction temperatures.

The magnitude of the change in the magnetic entropy is one of the measures to determine the applicability of the material for MCE applications. Another important measure is the relative cooling power (RCP) which is defined as "the amount of heat transferred between two temperatures", or refrigerant capacity (RC) which is defined as "amount of heat transfer between the hot and cold sinks in an ideal refrigeration cycle". RCP or RC depends on the magnitude of the change in the magnetic entropy between the two temperatures T_1 and T_2 and can be calculated according to the formula in Eq 2 [26,27]. Based on this equation we evaluated RCP between T_1 = 3.5 K (for x = 0.0) or 4.5 K (for

the rest of the samples) and $T_2 = 77.5$ K, using the magnitude of the change in magnetic entropy curves ($-\Delta S_M$ versus T).

$$RCP = \int_{T_1}^{T_2} |\Delta S_M| \, dT \tag{2}$$

The evaluated RCP values for the perovskite compounds as a function of yttrium composition (x) and as a function of the change in the applied magnetic field are shown in Figure 7. We can see from this figure that the compound with x = 0.0 has the largest value for the relative cooling power and x = 0.9 has the lowest value. What is interesting in this system of nanoparticle compounds that we have relatively large values (≈100 J/kg) for the RCP even at low values of the change in the applied magnetic field 1 to 2 T).

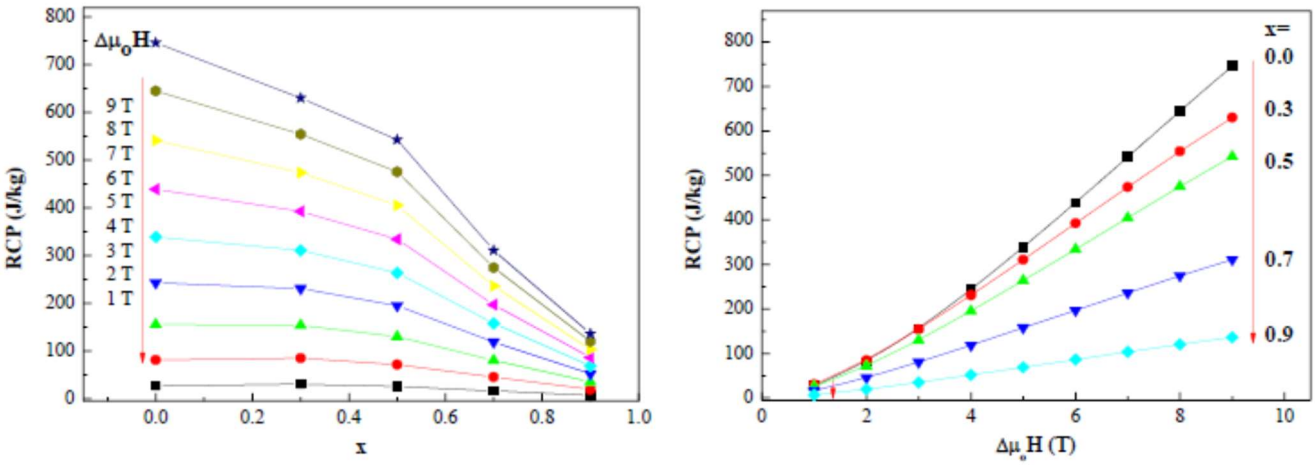

Figure 7. Dependence of the relative cooling power (refrigerant capacity) on the Y composition (x) and on the different values of the change in the applied magnetic field ($\Delta\mu_o H$) for the different $Gd_{1-x}Y_xCrO_3$ ($0.0 \leq x \leq 0.9$) nanoparticles.

To better understand and establish the relation between the magnitude of the change in the magnetic entropy and the change in the applied magnetic field we can assume $|\Delta S_M|$ depends on $(\Delta H)^n$, based on the analysis by Franco et al. [28,29] using the mean field theory yield $n \approx 1$ for $T < T_C$ to $n \approx 2$ for $T > T_C$.

Figure 8 shows the relation between $\ln|\Delta S_M|$ and lnH for the different compositions of yttrium, x. The solid lines represent the linear fitting to the experimental data. The slopes of the straight lines, gives the value of n, at T = 4.5 K are 1.5 ±0.2 (for x = 0.0) and 0.9 ±0.2 (for x = 0.3 to 0.9), while at T = 8.5 K they are 1.2 ±0.2 (for x = 0.0) and 0.9 ±0.2 (for x = 0.3 to 0.9). The values of n for all the nanoparticle compounds agree with the expected value and agree with the previously published values of 1.3 to 1.6 at temperatures below 20 K for $GdCrO_3$ by Shi et al. [27].

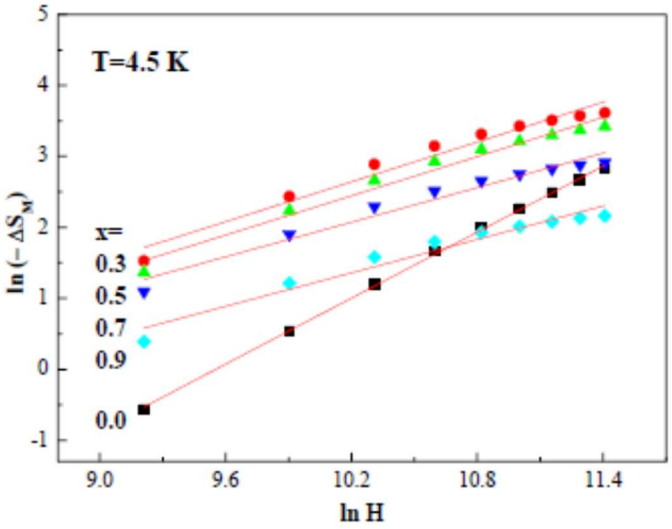

Figure 8. Dependence of ln (negative the change of magnetic entropy) on ln (the change in the applied magnetic field) for the different $Gd_{1-x}Y_xCrO_3$ ($0.0 \leq x \leq 0.9$) nanoparticles. The solid lines represent the linear fitting.

To shed light and to get deeper insight of the order of magnetic phase transition one can use Arrott plots. Using the data of the isotherm's magnetization curves (magnetization (M) as a function of the external field (H), we determined M^2 and H/M, then we plotted Arrott plots (M^2 versus H/M) as shown in Figure 9 for the different nanoparticle compounds. From the slope of the curves of Arrott plots [18], the order parameter of the magnetic transition can be estimated. At low temperature, all the curves show a downward concave curvature and as we increase the temperature the plots are displaced to the right and then at higher temperatures the curves become straight upwards. All the curves in an applied magnetic field up to 9 T show a positive slope reveals that the canted-antiferromagnetic to paramagnetic phase transition is second-order in nature. A negative slope usually represents a first order magnetic transition, which was not found in our system of nanoparticles.

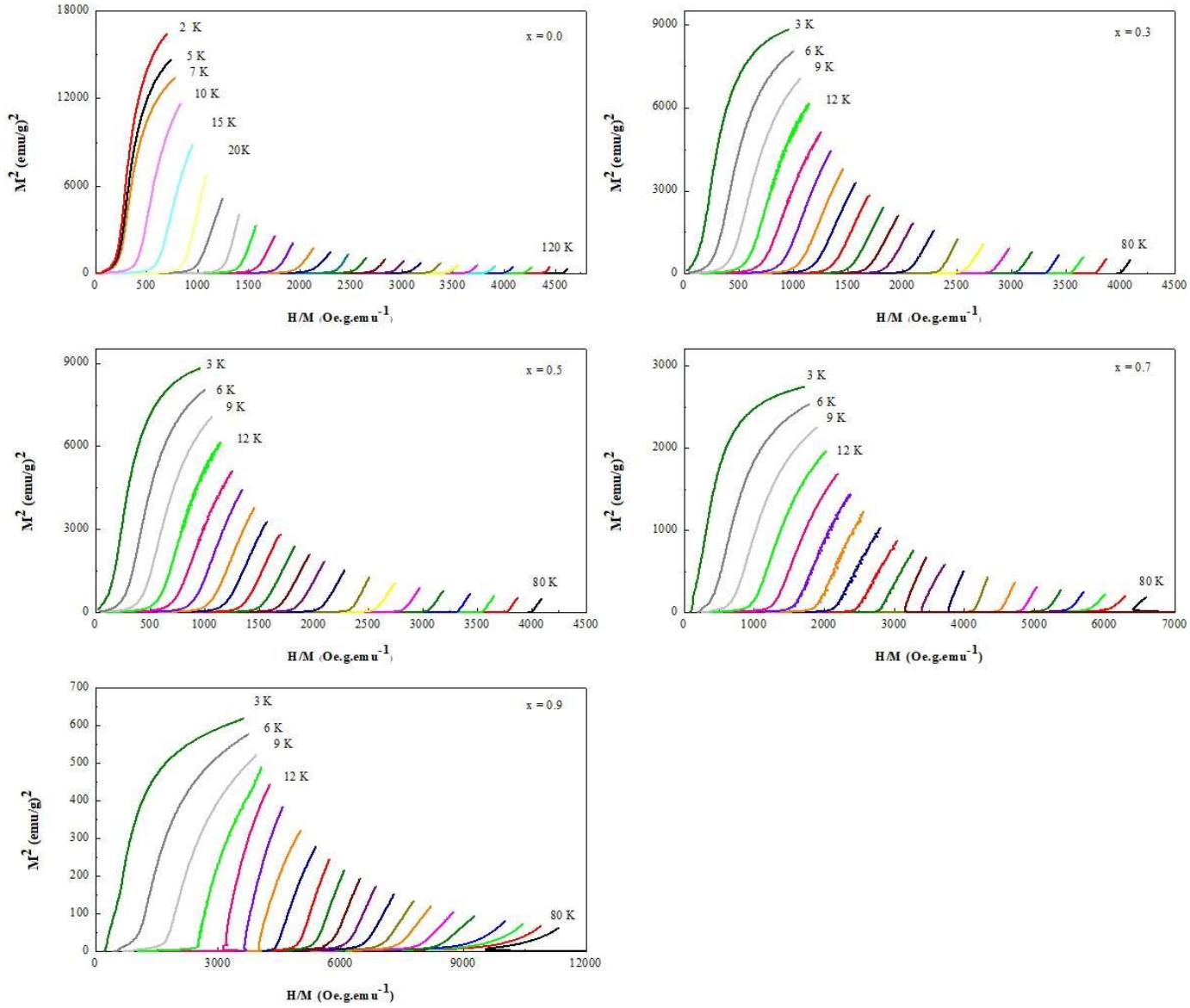

Figure 9. Arrott plots (M^2 versus H/M at different temperatures and for different Y compositions) for the different $Gd_{1-x}Y_xCrO_3$ ($0.0 \leq x \leq 0.9$) nanoparticles.

The magnetic behavior of the studied samples changes from canted antiferromagnetic below the ordering temperature of Cr^{3+} (T_N) to paramagnetic above T_N (which is between 145 and 170 K for the different compounds investigated in this study). The Gd^{3+} ordering temperature in $GdCrO_3$ single crystal is 2.3 K (which is below our measured range). The orbital angular momentum (L) for Gd^{3+} ions is zero, so the contribution to the total angular momentum (J) comes from the spin angular momentum (S = 7/2).

Due to this, the contribution to the magneto crystalline anisotropy from the crystal field effect can be neglected which makes the magnetization almost isotropic and large in our compounds [19–21]. The giant magnitude of the change in the magnetic entropy may be attributed mainly to the Gd^{3+}–Gd^{3+} interaction and partially due to magnetic entropy induced by the spin-reorientation of Cr^{3+} and Gd^{3+}

ions due to the Cr^{3+}–Gd^{3+} magnetic interaction in the non-collinear canted-antiferromagnetic systems. In this study we found a maximum value of $-\Delta S_M$ 45.6 J/kg·K for x = 0.0 and $\mu_o H$ = 9 T at 8.5 K for $-\Delta S_M$, which is comparable with the value of 52.5 J/kg·K for $GdCrO_3$ single crystal reported by Das et al. [21]. For the MCE applications, it is important to have large values of the magnitude of the change in the magnetic entropy and a large value for the relative cooling power at an achievable low magnetic field, which can be produced by permanent magnets (in the range of 1–2 T). In our system of nanoparticles, we can see that a large values for $|\Delta S_M|$ (3–11 J/kg·K) and RCP (30 to 85 J/Kg) can be reached in a change in the applied magnetic field of 1 to 2 T.

5. Conclusion

In summary, we used the auto-combustion method followed by annealing at 700 ℃ to prepare the $Gd_{1-x}Y_xCrO_3$ perovskite nanoparticles compounds. We found that all the synthesized samples form nano-particles with diameters in the range (53–110 ±6) nm and crystallized into a distorted orthorhombic structure with the space group (Pbnm). We have systematically investigated the magnetic and MCE properties of the nanoparticle (Gd, Y)-chromites including the temperature-dependent, the magnetic field-dependent, and the composition-dependent. The giant values of $-\Delta S_M$ and RCP and the wider temperature range of $-\Delta S_M$ suggest that these compounds may be considered as magnetic refrigerants materials in the cryogenic range from helium-liquefaction up to hydrogen-liquefaction temperatures.

Acknowledgments

Al-Omari would like to thank Sultan Qaboos University for the support provided during this study under the grant number IG /SCI/PHYS/20/05. We would like to thank Mr. Abdul Rahman Al-Nabhani for the help in TEM measurements, and the CAARU team for the XRD measurements.

Conflict of interest

The authors declare no competing interests.

References

1. Smith A, Bahl CRH, Bjørk R, et al. (2012) Materials challenges for high performance magnetocaloric refrigeration devices. *Adv Energy Mater* 2: 1288–1318. https://doi.org/10.1002/aenm.201200167
2. Dhahri K, Dhahri N, Dhahri J, et al. (2018) Critical phenomena and estimation of the spontaneous magnetization from a mean field analysis of the magnetic entropy change in $La_{0.7}Ca_{0.1}Pb_{0.2}Mn_{0.95}Al_{0.025}Sn_{0.025}O_3$. *RSC Adv* 8: 3099–3107. https://doi.org/10.1039/C7RA12827D
3. Nordblad P (2013) Strained relations. *Nat Mater* 12: 11–12. https://doi.org/10.1038/nmat3516

4. Zhao HJ, Íñiguez J, Chen XM, et al. (2016) Origin of the magnetization and compensation temperature in rare-earth orthoferrites and orthochromates. *Phys Rev B* 93: 014417. https://doi.org/10.1103/PhysRevB.93.014417
5. Gupta P, Bhargava R, Poddar P (2015) Colossal increase in negative magnetization, exchange bias and coercivity in samarium chromite due to a strong coupling between Sm^{3+}–Cr^{3+} spins sublattices. *J Phys D* 48: 025004. https://doi.org/10.1088/0022-3727/48/2/025004
6. Gupta P, Bhargava R, Das R, et al. (2013) Static and dynamic magnetic properties and effect of surface chemistry on the morphology and crystallinity of $DyCrO_3$ nanoplatelets. *RSC Adv* 3: 26427–26432. https://doi.org/10.1039/c3ra43088j
7. Bhadram VS, Rajeswaran B, Sundaresan A, et al. (2013) Spin-phonon coupling in multiferroic $RCrO_3$ (R-Y, Lu, Gd, Eu, Sm): a Raman study. *Eur Phys Lett* 101: 17008. https://doi.org/10.1209/0295-5075/101/17008
8. Yoshii K (2012) Magnetization reversal in $TmCrO_3$. *Mater Res Bull* 47: 3243–3248. https://doi.org/10.1016/j.materresbull.2012.08.005
9. Yoshii K, Nakamura A (2000) Reversal of magnetization in $La_{0.5}Pr_{0.5}CrO_3$. *J Solid State Chem* 155: 447–450. https://doi.org/10.1006/jssc.2000.8943
10. Gupta P, Poddar P (2015) Temperature and magnetic field-assisted switching of magnetization and observation of exchange bias in $YbCrO_3$ Nanocrystals. *Inorg Chem* 54: 9509–9516. https://doi.org/10.1021/acs.inorgchem.5b01448
11. Cao Y, Cao S, Ren W, et al. (2014) Magnetization switching of rare earth orthochromite $CeCrO_3$. *Appl Phys Lett* 104: 232405. https://doi.org/10.1063/1.4882642
12. Yusuf SM, Kumar A, Yakhmi JV (2009) Temperature-and magnetic-field-controlled magnetic pole reversal in a molecular magnetic compound. *Appl Phys Lett* 95: 182506. https://doi.org/10.1063/1.3259652
13. Prejbeanu IL, Kerekes M, Sousa RC, et al. (2007) Thermally assisted MRAM. *J Phys Condens Matter* 19: 165218. https://doi.org/10.1088/0953-8984/19/16/165218
14. Mahana S, Manju U, Topwal D (2018) $GdCrO_3$: a potential candidate for low temperature magnetic refrigeration. *J Phys D* 51: 305002. https://doi.org/10.1088/1361-6463/aacc98
15. Zhu Y, Zhou P, Li T, et al. (2020) Enhanced magnetocaloric effect and magnetic phase diagrams of single-crystal $GdCrO_3$. *Phys Rev B* 102: 144425. https://doi.org/10.1103/PhysRevB.102.144425
16. Oliveira GNP, Pires AL, Machado P, et al. (2019) Effect of chemical pressure on the magnetocaloric effect of perovskite-like $RCrO_3$ (R-Yb, Er, Sm and Y). *J Alloys Compd* 797: 269–276. https://doi.org/10.1016/j.jallcom.2019.05.011
17. Oliveira GNP, Machado P, Pires AL, et al. (2016) Magnetocaloric effect and refrigerant capacity in polycrystalline $YCrO_3$. *J Phys Chem Solids* 91: 182–188. https://doi.org/10.1016/j.jpcs.2015.12.012
18. Arrott A (1957) Criterion for ferromagnetism from observations of magnetic isotherms. *Phys Rev* 108: 1394. https://doi.org/10.1103/PhysRev.108.1394
19. Skomski R, Sellmyer DJ (2009) Anisotropy of rare-earth magnets. *J Rare Earth* 27: 675–679. https://doi.org/10.1016/S1002-0721(08)60314-2

20. Gorodetsky G, Treves D (1964) Second-Order susceptibility terms in orthoferrites at room temperature. *Phys Rev* 135: A97. https://doi.org/10.1103/PhysRev.135.A97
21. Das M, Roy S, Mandal P (2017) Giant reversible magnetocaloric effect in a multiferroic $GdFeO_3$ single crystal. *Phys Rev B* 96: 174405. https://doi.org/10.1103/PhysRevB.96.174405
22. Dalal B, Sarkar B, Ashok VD, et al. (2018) Magnetization reversal, exchange interaction, and switching behavior studies on Ru doped $GdCrO_3$. *J Alloys Compd* 739: 418–424. https://doi.org/10.1016/j.jallcom.2017.12.222
23. Shi C, Su Y, Guo J, et al. (2021) The microstructure and magnetic properties of Ca^{2+} ion doped $GdCrO_3$. *Ceram Int* 47: 10887–10892. https://doi.org/10.1016/j.ceramint.2020.12.208
24. Sardar K, Lees MR, Kashtiban RJ, et al. (2011) Direct hydrothermal synthesis and physical properties of rare-earth and yttrium orthochromite perovskites. *Chem Mater* 23: 48–56. https://doi.org/10.1021/cm102925z
25. Yoshii K (2019) Spin rotation, glassy state, and magnetization switching in R CrO_3 (R = $La_{1-x}Pr_x$, Gd, and Tm): Reinvestigation of magnetization reversal. *J Appl Phys* 126: 123904. https://doi.org/10.1063/1.5116205
26. Kumar S, Coondoo I, Vasundhara M, et al. (2017) Magnetization reversal behavior and magnetocaloric effect in $SmCr_{0.85}Mn_{0.15}O_3$ chromites. *J Appl Phys* 121: 043907. https://doi.org/10.1063/1.4974737
27. Shi J, Sauyet T, Dang Y, et al. (2021) Structure-property correlations and scaling in the magnetic and magnetocaloric properties of $GdCrO_3$ particles. *J Phys Condens Matter* 33: 205801. https://doi.org/10.1088/1361-648X/abf19a
28. Franco V, Conde A (2010) Scaling laws for the magnetocaloric effect in second order phase transitions: From physics to applications for the characterization of materials. *Int J Refrig* 33: 465–473. https://doi.org/10.1016/j.ijrefrig.2009.12.019
29. Franco V, Conde A, Romero-Enrique JM, et al. (2008) A universal curve for the magnetocaloric effect: an analysis based on scaling relations. *J Phys Condens Matter* 20: 285207. https://doi.org/10.1088/0953-8984/20/28/285207

AIMS Press